

Features of transport induced by ion-driven trapped-electron modes in tokamak plasmas

Hui Li(李慧), Ji-Quan Li(李继全), Feng Wang(王丰), Qi-Bin Luan(栾其斌),Hong-En Sun(孙宏恩), and Zheng-Xiong Wang(王正汹)

Citation: Chin. Phys. B, 2023, 32 (**7**): 075206. DOI: 10.1088/1674-1056/acae7e
Journal homepage: http://cpb.iphy.ac.cn; http://iopscience.iop.org/cpb

What follows is a list of articles you may be interested in

Role of the zonal flow in multi-scale multi-mode turbulence with small-scale shear flow in tokamak plasmas

Hui Li(李慧), Jiquan Li(李继全), Zhengxiong Wang(王正汹), Lai Wei(魏来), and Zhaoqing Hu(胡朝清)
Chin. Phys. B, 2022, 31 (**6**): 065207. DOI: 10.1088/1674-1056/ac6011

The intermittent excitation of geodesic acoustic mode by resonant Instanton of electron drift wave envelope in L-mode discharge near tokamak edge

Zhao-Yang Liu(刘朝阳), Yang-Zhong Zhang(章扬忠), Swadesh Mitter Mahajan, A-Di Liu(刘阿娣), Chu Zhou(周楚), and Tao Xie(谢涛)
Chin. Phys. B, 2022, 31 (**4**): 045202. DOI: 10.1088/1674-1056/ac43ac

Basic features of the multiscale interaction between tearing modes and slab ion-temperature-gradient modes

L Wei(魏来), Z X Wang(王正汹), J Q Li(李继全), Z Q Hu(胡朝清), Y Kishimoto(岸本泰明)
Chin. Phys. B, 2019, 28 (**12**): 125203. DOI: 10.1088/1674-1056/ab5437

Effect of Bohm quantum potential in the propagation of ion-acoustic waves in degenerate plasmas

M M Hasan, M A Hossen, A Rafat, A A Mamun
Chin. Phys. B, 2016, 25 (**10**): 105203. DOI: 10.1088/1674-1056/25/10/105203

Numerical study of the effect of water content on OH production in a pulsed-dc atmospheric pressure helium-air plasma jet

Mu-Yang Qian(钱沐杨), Cong-Ying Yang(杨从影), Zhen-dong Wang(王震东), Xiao-Chang Chen(陈小昌), San-Qiu Liu(刘三秋), De-Zhen Wang(王德真)
Chin. Phys. B, 2016, 25 (**1**): 015202. DOI: 10.1088/1674-1056/25/1/015202

SPECIAL TOPIC — Plasma disruption

Features of transport induced by ion-driven trapped-electron modes in tokamak plasmas

Hui Li(李慧)[1], Ji-Quan Li(李继全)[2], Feng Wang(王丰)[1,†], Qi-Bin Luan(栾其斌)[3], Hong-En Sun(孙宏恩)[3], and Zheng-Xiong Wang(王正汹)[1,‡]

[1] *Key Laboratory of Materials Modification by Laser, Ion, and Electron Beams (Ministry of Education), School of Physics, Dalian University of Technology, Dalian* 116024, *China*

[2] *Southwestern Institute of Physics, Chengdu* 610041, *China*

[3] *Faculty of Electronic Information and Electrical Engineering, Dalian University of Technology, Dalian* 116024, *China*

(Received 23 September 2022; revised manuscript received 14 December 2022; accepted manuscript online 27 December 2022)

As an obstacle in high-performance discharge in future fusion devices, disruptions may do great damages to the reactors through causing strong electromagnetic forces, heat loads and so on. The drift waves in tokamak are illustrated to play essential roles in the confinement performance as well. Depending on the plasma parameters and mode perpendicular wavelength, the mode phase velocity is either in the direction of electron diamagnetic velocity (namely, typical trapped electron mode) or in the direction of ion diamagnetic velocity (namely, the ubiquitous mode). Among them, the ubiquitous mode is directly investigated using gyro-fluid simulation associating with gyro-fluid equations for drift waves in tokamak plasmas. The ubiquitous mode is charactered by the short wavelength and propagates in ion diamagnetic direction. It is suggested that the density gradient is essential for the occurrence of the ubiquitous mode. However, the ubiquitous mode is also influenced by the temperature gradients and other plasma parameters including the magnetic shear and the fraction of trapped electrons. Furthermore, the ubiquitous mode may play essential roles in the turbulent transport. Meanwhile, the relevant parameters are scanned using a great number of electrostatic gyro-fluid simulations. The stability map is taken into consideration with the micro-instabilities contributing to the turbulent transport. The stability valley of the growth rates occurs with the assumption of the normalized temperature gradient equaling to the normalized density gradient.

Keywords: drift waves, nonlinear phenomena, plasma simulation

PACS: 52.35.Kt, 52.35.Mw, 52.65.–y **DOI:** 10.1088/1674-1056/acae7e

1. Introduction

Turbulent transport seriously impacts and restricts plasma confinement performance in magnetic fusion reactors.[1–3] In high-temperature fusion plasma, the energy transport across magnetic field lines including the particle and thermal transport greatly depends on the collective modes in regimes of the collisional mean free path longer than the relevant magnetic connection length. As one of the major issues in fusion plasma, disruptions are extremely dangerous. In the tokamak, as a well-known conception of disruption, the plasma can suddenly escape the confinement. This abrupt loss of confinement causes thermal and magnetic loads on the walls, as well as the potential formation of electron currents with relativistic energies, which can seriously damage the devices. To be a viable design for a fusion power plant, the tokamak must be able to avoid, or at least reliably mitigate, the effects of disruptions. Even without a power plant, the requirement of minimizing disruptions in ITER is essential.[4–6] Because the avoidance and mitigation techniques are inherently more effective when more warning time is provided for them to be implemented, much more attention has been paid to the disruption prediction.

It has been accepted that the magnetohydrodynamics (MHD) instabilities are related to the disruption.[7,8] Current-driven magnetohydrodynamics (MHD) instabilities, which are known as relating to the magnetic reconnection, are usually observed in both laboratory and space plasmas. However, it is unclear how the macro-scopic current-driven instabilities can couple to the microscopic magnetic reconnection, previous researches in the theory and simulation have revealed that the cascade via a transition of successively smaller scale current-driven instabilities is possible. In the previous experimental and numerical researches, the results demonstrate a viable path from macro-scale MHD physics to micro-scale non-MHD physics associated with the occurrence of fast reconnection.[9] In the last decade, the increasement of interest in the interaction between turbulence and MHD phenomena has occurred in the fusion device plasmas, both experimentally and theoretically.[10,11] The sawtooth and neoclassical tearing modes (NTMs) essentially dominate the core MHD activity.[12,13] The latter one can be made unstable by the current or nonlinearly seeded by the turbulence, edge localized modes (ELMs), or internal kink mode crashes.

†Corresponding author. E-mail: fengwang@dlut.edu.cn

‡Corresponding author. E-mail: zxwang@dlut.edu.cn

© 2023 Chinese Physical Society and IOP Publishing Ltd

Particularly in plasma core, much of the transport is due to the turbulence induced by the ion temperature gradient (ITG) mode and trapped electron mode (TEM).[14–16] Meanwhile, a critical physical model is built numerically to illustrate the anomalous particle convection reversal caused by ITG and TEM instabilities.[17] It has been generally recognized that ITG and TEM are responsible for the ion and electron transport, respectively.[18,19] However, there are interesting and important differences between these modes in tokamaks and stellarators. Several tokamaks, such as the Tore Supra,[20] KSTAR[21] and HL-2A devices,[22] have shown the evidence about the transition of turbulence including the ITG and/or TEM. The anomalous transport caused by micro-turbulence has been revealed recently including both in H-mode[23,24] and L-mode[25] plasmas. In additional, several physical effects, including the collisions, magnetic shear, finite β and finite Larmor radius effects[26–32] and other plasma parameters are considered as well. Furthermore, the turbulent transport is determined by the type of micro-turbulence[33,34] and it has been illustrated in the experiments, theories and simulations. Additional, transitions of turbulence in plasma density limits were discussed.[35] It is worthy to note the turbulent transport may also have influence on plasma disruptions, such as heavy impurity concentration to core region. TEM may adjust the heavy impurity pumping out.

The ubiquitous mode, as an important branch of trapped electron modes (TEMs), is a favored topic for studying anomalous energy transport in the fusion plasmas. On the one hand, typical TEMs have moderated to long wavelengths that propagate with the direction of electron diamagnetic drift. On the other hand, another essential branch of TEMs related to the $b_\mathrm{i} \equiv k_y^2\rho_\mathrm{i}^2/2 \gg 1$ is defined as the ubiquitous mode, which propagates in the direction of the ion diamagnetic drift velocity. Here, $\rho_\mathrm{s} = \sqrt{2T_\mathrm{e}/m_\mathrm{i}}/\Omega_\mathrm{i}$ represents the averaged sound speed ion gyro-radius in which Ω_i is the ion gyro-frequency.[36,37] Furthermore, it is discovered that the influence of η_e and η_i on the ubiquitous mode is different from those on the typical TEM, namely, it is better for ubiquitous mode to occur at the lower η_e. Since ubiquitous mode can cause relatively high anomalous diffusion, it is well accepted the importance of ubiquitous mode in the magnetic confined plasma. Although ubiquitous mode generally causes less energy loss than that of the typical TEM, ITG, and ETG modes, with certain conditions, ubiquitous mode can still result in the significant heat transport, especially in the range of fluid-like instability. For this reason, the ubiquitous mode is a significant branch of TEMs and should receive more considerations in turbulent transport analysis.[38,39] Thereby, the characters of the ubiquitous mode and the influence on the transport have to be revealed. This research will help us to better reveal the physical characters of ubiquitous mode and the role of the ubiquitous mode in tokamak transport.

The purpose of this research is to present the physics of the ubiquitous mode in the collisionless plasma, which can result in relatively strong anomalous plasma diffusion. More precisely, the parameters of the ubiquitous mode in tokamak plasmas are illustrated with simulations in this work based on the gyrofluid equations of drift waves in inhomogeneous plasmas. At first, we confirm the majority of theoretical predictions made about ubiquitous mode, two of which are the proof that ubiquitous mode exists in tokamaks and the proof that the magnetic drifts of both trapped ions and electrons are the real driving forces behind the ubiquitous mode. Finally, the findings demonstrate that ubiquitous mode is typically inevitable in the tokamak plasmas with various parameter regimes and that their greater development rates are what cause ubiquitous mode to contribute to the electron transport. These findings will have an influence on the revealing of the characteristics of ubiquitous mode in tokamaks. Simulations are used to investigate the space of profiles with $T_\mathrm{e}/T_\mathrm{i} = 1$. Finally, the results show a transition between the ion temperature gradient (ITG) instability and TEM, associated with a stability valley of the growth rates with significantly reduced growth rates.

The remainder of the paper is organized as follows. The physical model with relevant equations and the simulation setting will be introduced in Section 2. In Section 3, the numerical linear and nonlinear results will be brought in and systematically analyzed. The electrostatic stability map is presented in this section as well. In Section 4, we will provide a summary of our findings as well as some discussions.

2. Physical model and simulation setting

To simulate the time evolution of the ion-driven trapped-electron mode and understand the underlying mechanism of the nonlinear turbulent transport, a set of five-field fluid equations is advanced based on the Weiland model[40] here. The effects of both the Landau damping effect[41–43] and the non-adiabatic response of trapped electrons are included in this model for describing the evolution of global electrostatic ITG and TEM turbulence through exploiting the extended fluid code (ExFC) based on the so-called Landau–Fluid model as follows:

$$d_t n_\mathrm{e} = -\omega_\mathrm{dte}\left(n_0\phi - T_{\mathrm{e}0}n_\mathrm{e} - n_0 T_\mathrm{e}\right) + D_n\nabla_\perp^2 n_\mathrm{e}, \tag{1}$$

$$\begin{aligned} d_t T_\mathrm{e} = &-T_{\mathrm{e}0}\omega_\mathrm{dte}\left[(\varsigma-1)(\phi - \tau_\mathrm{en}n_\mathrm{e}) - (2\varsigma-1)T_\mathrm{e}\right] \\ &-(\varsigma-1)\sqrt{8m_\mathrm{e}T_{\mathrm{e}0}/m_\mathrm{i}\pi}\left|\nabla_\parallel\right|T_\mathrm{e} + D_{T_\mathrm{e}}\nabla_\perp^2 T_\mathrm{e}, \end{aligned} \tag{2}$$

$$\begin{aligned} d_t\Omega = &-T_{\mathrm{i}0}a\left(\partial_r \ln n_0 + \partial_r \ln T_{\mathrm{i}0}\right)\partial_\theta\nabla_\perp^2\phi \\ &+ f_\mathrm{c}a\partial_r \ln n_0\partial_\theta\phi - \nabla_\parallel \upsilon_\parallel \\ &+ \omega_\mathrm{di}\left[(1+f_\mathrm{c}/\tau)\phi + T_\mathrm{i} + f_\mathrm{t}\tau_\mathrm{in}n_\mathrm{e}\right] \\ &+ f_\mathrm{t}\omega_\mathrm{dte}\left(\phi - T_\mathrm{e} - \tau_\mathrm{en}n_\mathrm{e}\right) + D_U\nabla_\perp^2\Omega, \end{aligned} \tag{3}$$

$$d_t \upsilon_\parallel = -\nabla_\parallel T_\mathrm{i} - f_\mathrm{t}\tau_\mathrm{in}\nabla_\parallel n_\mathrm{e} - (1+f_\mathrm{c}/\tau)\nabla_\parallel \phi + D_\upsilon \nabla_\perp^2 \upsilon_\parallel, \quad (4)$$

$$\begin{aligned} d_t T_\mathrm{i} = & -T_{\mathrm{i}0}(\varsigma-1)\nabla_\parallel \upsilon_\parallel \\ & + T_{\mathrm{i}0}\omega_\mathrm{di}\{(\varsigma-1)[(1+f_\mathrm{c}/\tau)\phi + f_\mathrm{t}\tau_\mathrm{in} n_\mathrm{e}] + (2\varsigma-1)T_\mathrm{i}\} \\ & - (\varsigma-1)\sqrt{8T_{\mathrm{i}0}/\pi}\left|\nabla_\parallel\right| T_\mathrm{i} + D_{T_\mathrm{i}}\nabla_\perp^2 T_\mathrm{i}, \end{aligned} \quad (5)$$

where n_e, T_e, Ω, $\upsilon_\parallel$ and T_i are the normalized electron density, electron temperature, vorticity, parallel ion velocity and ion temperature, respectively, with the operators $d_t f = \partial_t f + [\phi, f]$ and $[\phi, f] = r^{-1}(\partial_r\phi\partial_\theta f - \partial_\theta\phi\partial_r f)$. Here, f represents any field variable. $\varsigma = 5/3$ represents the adiabatic compression index. The diffusivity terms are set as $D_n = D_{T_\mathrm{e}} = D_U = D_\upsilon = D_{T_\mathrm{i}} = 4.8\times10^{-3}$.

The other operators are written as $\omega_\mathrm{dte} = 2\varepsilon\lambda_t q r^{-1}\partial_\varphi$, $\omega_\mathrm{di} = 2\varepsilon\left(\cos\theta r^{-1}\partial_\theta + \sin\theta\partial_r\right)$ and $\lambda_t = 1/4 + 2s/3$, namely, the trapped electron precession drift operator, the ion magnetic drift operator and the dependence of the precession frequency of trapped electron on the magnetic shear $s = r\mathrm{d}q/q\mathrm{d}r$, respectively. And $\varepsilon = a/R$ is the inverse aspect ratio. The fraction of trapped electron is $f_\mathrm{t} = 2\sqrt{2r/R}/\pi$ and the passing electron is set as $f_\mathrm{c} = 1 - f_\mathrm{t}$. The parallel velocity of trapped electron is set as homogenous. In ExFC code, the real frequency of the TEM is positive.

The normalization of the gyroBohm type is as follows:

$$\left(t\frac{c_{\mathrm{s}0}}{a}, \frac{r}{\rho_{\mathrm{s}0}}, \rho_{\mathrm{s}0}\nabla_\perp, a\nabla_\parallel\right) \to \left(t, r, \nabla_\perp, \nabla_\parallel\right), \quad (6)$$

$$\frac{a}{\rho_{\mathrm{s}0}}\left(\frac{n_\mathrm{e}}{n_0}, \frac{T_\mathrm{e}}{T_{\mathrm{e}0}}, \frac{e\phi}{T_{\mathrm{e}0}}, \frac{\upsilon_\parallel}{c_{\mathrm{s}0}}, \frac{T_\mathrm{i}}{T_{\mathrm{i}0}}\right) \to \left(n_\mathrm{e}, T_\mathrm{e}, \phi, \upsilon_\parallel, T_\mathrm{i}\right), \quad (7)$$

where the ion sound gyroradius $\rho_{\mathrm{s}0} = m_\mathrm{i}c_{\mathrm{s}0}/e_\mathrm{i}B_0$ and the ion sound speed $c_{\mathrm{s}0} = (T_{\mathrm{i}0}/m_\mathrm{i})^{1/2}$. The unit of the transport coefficient is $\rho_{\mathrm{s}0}^2 c_{\mathrm{s}0}/a$. The ratios of the temperature and density are shown as

$$\tau = T_{\mathrm{e}0}/T_{\mathrm{i}0}, \quad \tau_\mathrm{en} = T_{\mathrm{e}0}/n_0, \quad \tau_\mathrm{in} = T_{\mathrm{i}0}/n_0. \quad (8)$$

The equilibrium quantity in unit of arbitrary reference value is represented by the subscript label with 0.

The nonlinear Eqs. (1)–(5) are numerically solved in usual toroidal coordinate (r, θ, φ). The simulation is set in the range $[L_r, L_\theta, L_\varphi] \approx [a, 2\pi, 2\pi]$. The corresponding grid points are $[N_x, N_y, N_z] = [128, 256, 128]$. The global effects of plasma profiles which may have influence on the growth rate of the fluctuation are considered. In the research, the parametric profiles are applied in simulations as the density profiles

$$n_0(r) = n_\mathrm{c}\exp\{-(\Delta_r/L_n)\tanh[(r-r_0)/\Delta_r]\}, \quad (9)$$

the temperature profiles

$$T_{s0}(r) = T_{s\mathrm{c}}\exp\{-(\Delta_{rs}/L_{T_s})\tanh[(r-r_0)/\Delta_{rs}]\}, \quad (10)$$

and the safety factor

$$q(r) = q_0 + q_a(r/a)^2. \quad (11)$$

Here, the subscript label s stands for the species of electron and ion, the label c corresponds to the plasma center with magnetic axis. The other parameters are $r_0 = 0.5a$ and $\Delta_r = \Delta_{rs} = 0.15a$. Further details and benchmarks of the ExFC can be found in our previous work as Refs. [44,45]. In the following simulation, except for the additional statement $T_\mathrm{e} \sim T_\mathrm{i}$ and $\eta_\mathrm{i} \approx \eta_\mathrm{e} = 0.4$.

3. Numerical simulation and modeling analysis

3.1. Parameter dependence

In this section, we discover the TEMs with two branches by examining the wavenumber spectra of low frequency drift waves through the gyro-fluid simulations. In the lower k_θ regime, the real frequency ω is positive indicating a typical TEM branch propagating with the electron diamagnetic drift direction as shown in Fig. 2. However, in the higher k_θ regime, the real frequency turns into negative regime which represents the instability is in the ion diamagnetic drift direction. The tokamak parameter, such as the inverse aspect ratio ε, influences the appearance of the ubiquitous mode and the intensity of the instabilities. It is obviously displayed in Fig. 1 in which the growth rates are enhanced with the increment of the ε. The threshold of the ubiquitous mode is influenced as well. It is suggested that the toroidal number for the ubiquitous mode excited drops significantly associated with the inverse aspect ratio increasing. The result implies that it is easy for the TEM changing into the regime of ubiquitous mode with

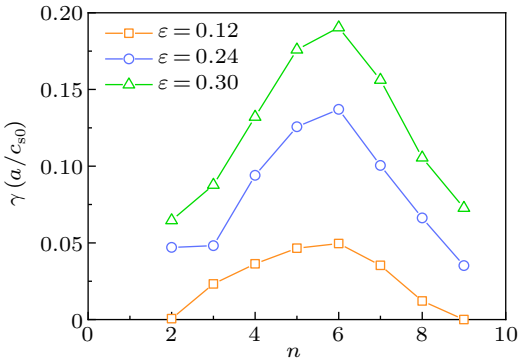


Fig. 1. The normalized growth rate with the functions of toroidal wavenumber n as $\varepsilon = 0.12$, 0.24 and 0.3.

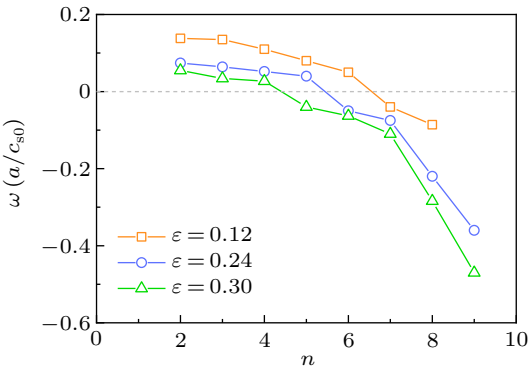


Fig. 2. The normalized frequency with the functions of toroidal wavenumber n as $\varepsilon = 0.12$, 0.24 and 0.3.

the increasement of the fraction of trapped electrons. Similar result is displayed in the research[39] with gyrokinetic simulations. With further searching, the nonlinear transports are displayed.

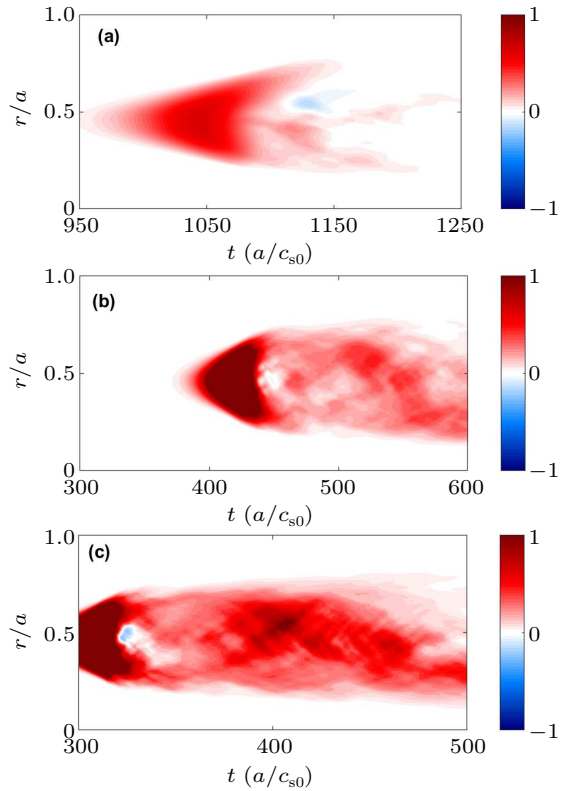


Fig. 3. Time evolution of radial particle flux Γ with (a) $\varepsilon = 0.12$, (b) $\varepsilon = 0.24$ and (c) $\varepsilon = 0.3$.

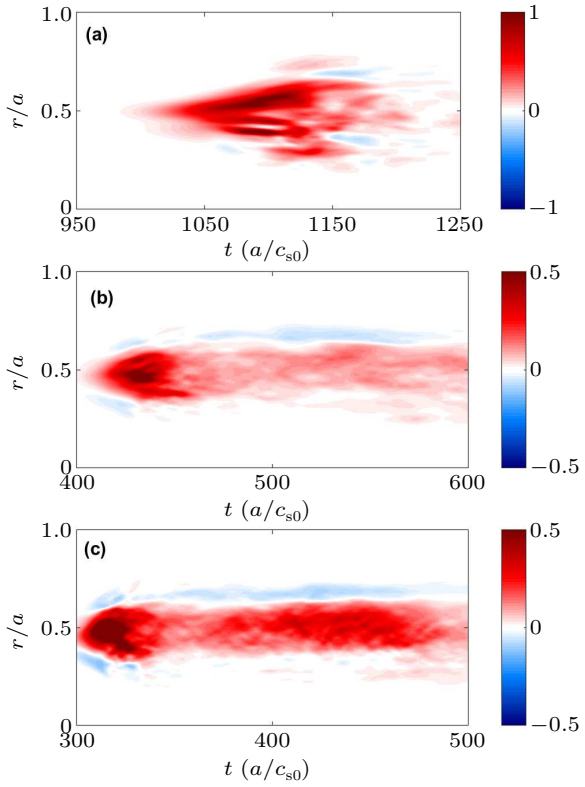


Fig. 4. Time evolution of ion heat flux Q_i with (a) $\varepsilon = 0.12$, (b) $\varepsilon = 0.24$ and (c) $\varepsilon = 0.3$.

As introduced in Section 1, the ubiquitous mode can cause relatively strong anomalous diffusion especially for the heat diffusions. Here, for instance, the evolutions of ion particle flux Γ and heat flux Q_i are displayed in Figs. 3 and 4. The outward particle flux is greatly enhanced as the ε increases. For the heat flux, the similar character is revealed. However, it is more localized for the heat flux compared with the particle flux. The effect of another plasma parameter, η_e, is also researched. Figures 5(a) and 5(b) represent that the ubiquitous mode has a threshold value and it increases with increasing η_e. It can be concluded that the typical TEM occurs with larger η_e. In other words, with η_e increasing, the ubiquitous mode turns into the typical TEM. It can be concluded that the higher ε and lower η_e are beneficial for the occurrence of the ubiquitous mode.

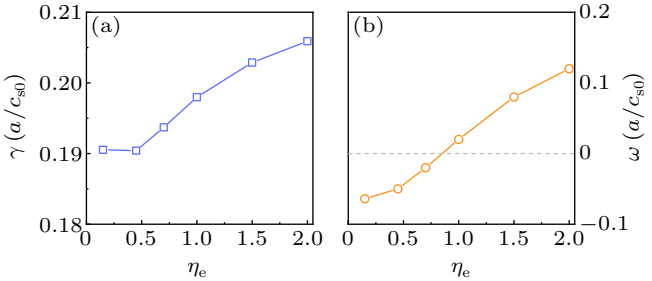


Fig. 5. (a) The normalized growth rate and (b) the normalized frequency with the functions of η_e with toroidal wavenumber $n = 7$.

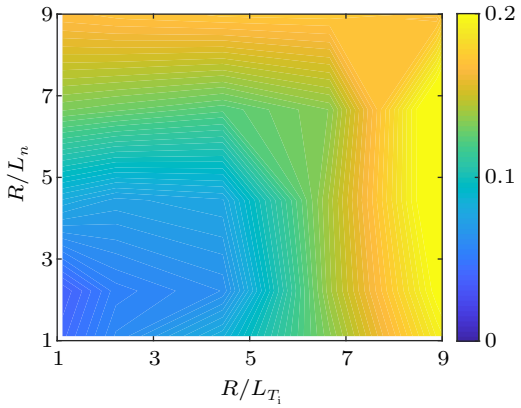


Fig. 6. Diagram for the growth rate of dominant instability depending on three key parameters $(R/L_n, R/L_{T_\mathrm{e}}, R/L_{T_\mathrm{i}})$. Here, $R/L_{T_\mathrm{e}} = R/L_{T_\mathrm{i}}$.

Here, the electrostatic stability map is presented as displayed in Fig. 6. The map is created with plotting the growth rate γ of the most unstable mode. The simulations are scanned with ion temperature gradient R/L_{T_i} and density gradient R/L_n. The temperature gradients of ion and electron are set as equal, namely $R/L_{T_\mathrm{i}} = R/L_{T_\mathrm{e}}$. In the Fig. 6, TEM is dominant on the top-left where R/L_n is greater than R/L_{T_i}. In the region $R/L_{T_\mathrm{i}} < R/L_n$, the dominant mode is ITG. Besides these two regions of the map, the mode is dominant mixed with ITG and TEM. As shown in Fig. 6, the monotonic increase of growth rate with higher temperature gradients is observed. As the density increases, the transition occurs from ITG to TEM. However, as shown in Fig. 7, there is a valley of the growth rate

around $\eta_i \sim 1$ as the R/L_n increases. In this region, the instability is mixed including both TEM and ITG with suppressed micro-instabilities.

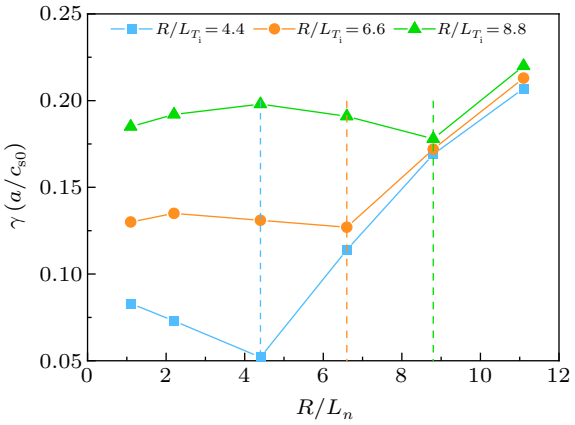


Fig. 7. Growth rates as a function of R/L_n. The dashed lines are $R/L_n = 4.4$ (blue), $R/L_n = 6.6$ (green) and $R/L_n = 8.8$ (orange). Here, $k_\theta = 0.34$ with $R/L_{T_i} = R/L_{T_e}$.

4. Summary

We investigate the properties of ubiquitous mode corresponding to the TEM using gyro-fluid simulation in collisionless plasmas. It is critical in revealing the anomalous transport. The ubiquitous mode obviously occurs in tokamaks which are provided by the findings. It is found that the ubiquitous mode drifts in the ion diamagnetic direction with short wavelength. It is displayed that the wavenumber for the ubiquitous mode changed into typical mode is influenced by the parameters. Furthermore, the ubiquitous mode may play essential roles in turbulent transport as well. Then, we investigate a region of the electrostatic instability space with the assuming of $R/L_{T_i} = R/L_{T_e}$. The growth rate decreases around the region $\eta_i \approx 1$ as the R/L_n increases accompanied with the coexistence of ITG and TEM. When the appropriate profile requirements are satisfied, the valley can create opportunities for operation with decreased losses associated with the assumption of the suppression of the micro-instabilities results in lower turbulent transport.

Acknowledgments

Project partially supported by the National Natural Science Foundation of China (Grant Nos. 12205035 and 11925501) and also partially by the National Key Research and Development Program of China (Grant Nos. 2017YFE0301200 and 2017YFE0301201).

References

[1] Hoang G T, Bourdelle C, Garbet X, *et al.* 2006 *Nucl. Fusion* **46** 306
[2] Guttenfelder W, Peterson J L, Candy J, Kaye S M, Ren Y, Bell R E, Hammett G W, LeBlanc B P, Mikkelsen D R, Nevins W M and Yuh H 2013 *Nucl. Fusion* **53** 093022
[3] Maeyama S, Idomura Y, Watanabe T H, Nakata M, Yagi M, Miyato N, Ishizawa A and Nunami M 2015 *Phys. Rev. Lett.* **114** 255002
[4] Schuller F C 1995 *Plasma Phys. Control. Fusion* **37** A135
[5] Hender T C, Wesley J C, Bialek J, Bondeson A, Boozer A H, Buttery R J, Garofalo A, Goodman T P, Granetz R S and Gribov Y 2007 *Nucl. Fusion* **47** S128
[6] de Vries P C, Pautasso G, Humphreys D, Lehnen M, Maruyama S, Snipes J A, Vergara A and Zabeo L 2016 *Fusion Sci. Technol.* **69** 471
[7] Zohm H, Maraschek M, Pautasso G, *et al.* 1995 *Plasma Phys. Control. Fusion* **37** A313
[8] Wang H H, Sun Y W, Shi T H, *et al.* 2020 *Nucl. Fusion* **60** 126008
[9] Seo B, Wongwaitayakornkul P, Haw M A, Ryan S M, Li H and Paul M B 2020 *Phys. Plasmas* **27** 022109
[10] Wei L, Wang Z X, Li J Q, Hu Z Q and Kishimoto Y 2019 *Chin. Phys. B* **28** 125203
[11] Wang Z, Tang W and Wei L 2022 *Plasma Sci. Technol.* **24** 033001
[12] Li J C, Dong J Q, Ji X Q and Hu Y J 2021 *Chin. Phys. B* **30** 075203
[13] Ji X Q, Yang Q W, Feng B B, Xu Y, Sun T F and Yuan B S 2011 *Chin. Phys. B* **20** 095205
[14] Petty C C and Luce T C 1994 *Nucl. Fusion* **34** 121
[15] Dong J Q and Horton W 1995 *Phys. Plasmas* **2** 3412
[16] Hu W, Feng H Y and Zhang W L 2019 *Chin. Phys. Lett.* **36** 085201
[17] Sun T T, Chen S Y, Wang Z H, Peng X D, Huang J, Mou M L and Tang C J 2015 *Chin. Phys. Lett.* **32** 035201
[18] Xiao Y and Lin Z 2009 *Phys. Rev. Lett.* **103** 085004
[19] Dimit A M, Bateman G, Beer M A, Cohen B I, Dorl W, Hammett G W, Kim C, Kinsey J E, Kotschenreuther M, Kritz A H, Lao L L, Mandrekas J, Nevins W M, Parker S E, Redd A J, Shumaker D E, Sydora R and Weiland J 2000 *Phys. Plasmas* **7** 969
[20] Arnichand H, Sabot R, Hacquin S, Krämer-Flecken A, Garbet X, Citrin J, Bourdelle C, Hornung G, Bernardo J, Bottereau C, Clairet F, Falchetto G and Giacalone J C 2014 *Nucl. Fusion* **54** 123017
[21] Lee W, Kwon J M, Ko S H, Leem J, Yun G S, Park H K, Park Y S, Kim K W and Luhmann N C 2018 *Phys. Plasmas* **25** 022513
[22] Zhong W L, Shi Z B, Yang Z J, Xiao G L, Yang Z C, Zhang B Y, Shi P W, Du H R, Pan X M, Zhou R B, Wan L H, Zou X L, Xu M, Duan X R, Liu Y, Zhuang G, HL-2A Team and J-TEXT Team 2016 *Phys. Plasmas* **23** 060702
[23] Mordijck S, Wang X, Doyle E J, Rhodes T L, Schmitz L, Zeng L, Staebler G M, Petty C C, Groebner R J, Ko W H, Grierson B A, Solomon W M, Tala T, Salmi A, Chrystal C, Diamond P H and McKee G R 2015 *Nucl. Fusion* **55** 113025
[24] Ryter F, Angioni C, Dunne M, Fischer R, Kurzan B, Lebschy A, McDermott R M, Suttrop W, Tardini G, Viezzer E, Willensdorfer M and the ASDEX Upgrade Team 2019 *Nucl. Fusion* **59** 096052
[25] Mariani A, Brunner S, Dominski J, Merle A, Merlo G, Sauter O, Gorler T, Jenko F and Told D 2018 *Phys. Plasmas* **25** 012313
[26] Candy J 2005 *Phys. Plasmas* **12** 072307
[27] Snyder P B and Hammett G W 2001 *Phys. Plasmas* **8** 744
[28] Snyder P B 1999 *Gyrofluid theory and simulation of electromagnetic turbulence and transport in tokamak plasmas* (Ph.D. Thesis) (Princeton: Princeton University)
[29] Kinsey J E, Waltz R E and Candy J 2006 *Phys. Plasmas* **13** 022305
[30] Weikl A, Peeters A G, Rath F, Grosshauser S R, Buchholz R, Hornsby W A, Seiferling F and Strintzi D 2017 *Phys. Plasmas* **24** 102317
[31] Mariani A, Brunner S, Merlo G and Sauter O 2019 *Plasma Phys. Control. Fusion* **61** 064005
[32] Han M K, Zhong W L, Dong J Q, *et al.* 2021 *Nucl. Fusion* **61** 046010
[33] Li H, Li J, Wang Z, Wei L, Hu Z and Ren G 2020 *Phys. Plasmas* **27** 082304
[34] Li H, Li J, Wang Z, Wei L and Hu Z 2022 *Chin. Phys. B* **31** 065207
[35] Xu X Q, Nevins W M, Rognlien T D, Bulmer R H, Greenwald M, Mahdavi A, Pearlstein L D and Snyderd P 2003 *Phys. Plasmas* **10** 5
[36] Coppi B and Rewoldt G 1974 *Phys. Rev. Lett.* **33** 1329
[37] Coppi B and Pegoraro F 1977 *Nucl. Fusion* **17** 969
[38] Coppi B and Rewoldt G 1974 *Phys. Lett.* **49** 36
[39] Shen Y, Dong J Q, Li J, Han M K, Li J Q, Sun A P and Qu H P 2019 *Nucl. Fusion* **59** 106011
[40] Nordman H, Weiland J and Jarmén A 1990 *Nucl. Fusion* **30** 983
[41] Beer M A 1995 *Gyrofluid models of turbulent transport in tokamaks* (Ph.D. Thesis) (Princeton: Princeton University)
[42] Garbet X, Garzotti L, Mantica P, Nordman H, Valovic M, Weisen H and Angioni C 2003 *Phys. Rev. Lett.* **91** 035001
[43] Garbet X, Dubuit N, Asp E, Sarazin Y, Bourdelle C, Ghendrih P and Hoang G T 2005 *Phys. Plasmas* **12** 082511
[44] Li H, Li J Q, Fu Y L, Wang Z X and Jiang M 2022 *Nucl. Fusion* **62** 036014
[45] Li J, *et al.* 2020 *IAEA Fusion Energy Conference*, 2020, Nice, pp. 7–21